Assessment of critical conditions for the onset of boiling on WCAC heat exchanger

Alexandre Ferreira Teixeira
a.ferreira.teixeira@tecnico.ulisboa.pt

Instituto Superior Técnico, Universidade de Lisboa, Portugal

December 2021

Abstract

The present work aims to design, assemble and test an experimental setup to characterise the critical conditions for the occurrence of boiling in a water charge air cooler intercooler and thus better understand this phenomenon. To carry out this study, a test section was designed and adapted to an experimental setup to simulate the operation of the heat exchanger and the necessary instrumentation for data collection was installed. The contact angles between the test surfaces, made of 3003 aluminium, and the liquids were determined to characterise their interaction. The roughness of the surfaces was measured, with a profilometer, to characterise their topography. Boiling tests were conducted with water and with a mixture of ethylene glycol and water (50/50 by volume) to understand if the test section and the experimental setup were able to identify, through different methods present in the literature, the onset of boiling and a comparison of the results obtained with the different methods was performed. It was concluded that the mixture needs a higher heat flux and a higher excess temperature to initiate boiling compared to water for the same experimental conditions. Boiling tests at mass flow rates of 3.5 kg/h, 5 kg/h and 10 kg/h were carried out, which showed that the excess temperature required for the onset of nucleate boiling increased with increasing mass flow rate. A high-speed camera was used to record the onset and different phases of nucleated boiling as well as the phenomenon of coalescence between bubbles. Overall the setup can be used to perform a detailed study on the critical conditions for the occurrence of boiling, for the established working conditions, for the heat exchanger of interest in the context of this study.
Keywords: Flow boiling, heat transfer, onset of nucleate boiling, water charge air cooler.

1. Introduction

The use of intercoolers, in turbocharged engines, increases the specific mass of air by lowering its temperature. As the specific output of a combustion engine is proportional to the specific mass of the inducted air, engine power can thus be increased.

Replacing air charge air cooler (ACAC) intercoolers with water charge air cooler (WCAC) intercoolers allows for greater equipment compactness. This brings numerous advantages in the automotive industry. Using WCAC intercooler means that there is less air volume between the turbo outlet and the admission valves, which means a smaller pressure drop and better engine response at transient regime. It also allows better thermal control of the air flow to the engine by controlling the coolant flow, something not possible with ACAC intercoolers where the coolant is the outside air. The use of WCAC intercoolers contributes to less architectural complexity and a reduction of up to 50% in the air intake circuit and, if the intercooler is coupled to the intake manifold, it is possible to eliminate the air tube connecting the outlet of the intercooler to the engine admission [1]. By reducing the air intake circuit volume, the pressure drop is also reduced, allowing the turbocharger to do less work while maintaining the same pressure at the engine inlet. This allows the flow rate of gases to the turbine to be lower and, consequently, the turbine temperature and exhaust gas pressure to decrease. On the other hand, the use of a WCAC intercooler implies the addition of a circuit for the coolant and a pump which can be driven electrically or by mechanical action from the engine to ensure the flow of coolant through the circuit. This work recreates experimentally the operation of a WCAC to determine the critical conditions for the occurrence of the boiling of the coolant and thus to understand the operating limitations of this type of equipment.

1.1. State of art

Determining the onset of nucleate boiling is of high interest in various engineering applications, especially when trying to protect equipment from flow instabilities and maximum heat fluxes that may cause damage to the equipment.

The boiling phenomenon was first studied by Nukiyama [2] who verified different boiling regimes for a quiescent medium. By measuring the voltage difference and the intensity of the current flowing through a platinum wire in a container of water, Nukiyama created a boiling curve that demonstrates the relation between the heat flux, q", and the excess temperature ΔT_e.

Bergles and Rohsenow [3] carried out flow boiling tests. Its experimental installation allowed degassed water to flow through a horizontally positioned stainless steel tube. Connected to the tube was a DC power supply for heating the tube, by Joule effect. From this study it is shown that the flow boiling curve should not be based on data taken from boiling in quiescent medium.

In the automotive industry, ethylene glycol mixtures are used in WCAC intercoolers as well as engine coolants. Due to the high surface temperatures the heat transfer takes place through two-phase flow [4]. Kandlikar and Bulut [4] conducted a series of tests for different mixtures of ethylene glycol with water. The experiments were carried out in a 6061-T6 aluminium channel with a cross-section of $3 \times 40mm$ and with mixtures with 0 to 40% of ethylene glycol.

Lee and Cholewczynski [5] placed thermocouples inside a combustion engine cooled by a 50/50 mixture of ethylene glycol and water. The tests were performed on wide open throttle conditions with the engine running at 3000 and 5600 rpm. Experimental tests reported boiling for heat fluxes between 20 and 60 W/cm^2.

O'Neill [6] conducted tests with a mixture of ethylene glycol and water 50/50 in a horizontal rectangular channel heated from the bottom, with a cross-section $20 \times 30mm$ for flow velocities between 0.5 m/s and 4 m/s, pressure between 1 and 1.6 bar, subcooled temperatures between 10 and 50$°C$ and with heat fluxes between 0 and 80 W/cm^2. With an experimental installation with the purpose of reproducing the coolant circuit of a combustion engine, O'Neill was able to identify the nucleated boiling onset and plot the boiling curves for different operating conditions. Later, Lee and O'Neill [7] carried out tests, for the same conditions, on an explosion engine, 4-cylinder and 1600 cm^3 and obtained similar boiling curves using the engine and the experimental installation.

Yu et al [8] created an experimental setup to simulate the cooling circuit of heavy vehicle engines. The test section consisted of an AISI 1010 tube with an internal diameter of 10.9 mm heated, by Joule effect, by a DC power supply. The tests were carried out with a 40/60 and 50/50 mixture of ethylene glycol and water with flow velocities of 0.25 m/s and at atmospheric pressure. Tests with different liquid inlet temperatures verified the increase in the heat flux required to initiate boiling for lower inlet temperatures and consequently higher subcooling.

Cunha [9] inserted thermocouples inside a WCAC intercooler to obtain the temperatures of both working fluids and installed a sight glass at the intercooler outlet to quantify the boiling, on a scale of 0 to 5. This study considered tests for air inlet temperatures between 170$°C$ and 210$°C$, air mass flow rates between 350 kg/h and 1100 kg/h , liquid inlet temperatures between 45$°C$ and 75$°C$, liquid mass flow rates between $14L/min$ and $26L/min$ and liquid inlet pressures between $1.5barA$ and $3barA$. It was concluded that boiling was inevitable due to the high temperatures inside the equipment.

Yu et al [10] conducted boiling tests of mixtures of ethylene glycol with 50/50 water in rectangular aluminium finned channels with 1.75 mm width and 14 mm height at 2 atm pressure. Flow velocities from 0.8 m/s to 0.12 m/s were tested obtaining the respective boiling curves and heat transfer coefficients. The tests reported an increase in the heat transfer coefficient and an increase in the heat flux required for the ONB with increasing flow velocity.

In addition to the methods for identifying nucleated boiling onset, referred to in section 2, the work of De Yeong et al [11] who identified nucleated boiling onset and critical heat flux using acoustic signals is noteworthy.

2. Background

The onset of nucleated boiling marks the boundary between single-phase and two-phase heat transfer. Until the onset of nucleated boiling the heat transfer mechanism is forced convection and, after the onset of nucleated boiling, there is a combination of forced convection with boiling [12]. During single-phase heat transfer, the surface temperature and the excess temperature vary linearly with the heat flux. When the surface temperature exceeds the saturation temperature of the liquid and reaches a certain excess temperature, the first vapor bubbles appear. This phenomenon causes the surface temperature to remain constant, or even decrease, with the increase of heat flux. This causes the boiling curve to move away from the line of heat transfer by forced convection. Thus, the onset of nucleated boiling can be defined as the point at which the boiling curve departs from the line of forced convection [13].

The nucleated boiling onset occurs for a given excess temperature and heat flux, which depend on the contact angle, mass flow rate and liquid subcooling. By increasing the mass flow rate, the flow velocity is increased as the cross-sectional area remains constant. With increasing flow velocity, the thermal boundary layer thickness decreases, reducing the number of active cavities in the nucleation process.

The liquid subcooling, defined as $\Delta T_{sub} = T_{sat} - T_{in}$, quantifies the difference between the liquid temperature and the liquid saturation temperature. This parameter influences the incipience of boiling. Like with the increase of flow velocity, increasing subcooling decreases the number of active cavities.

Hong et al [13] and Basu et al [12] showed the differences in the ONB excess temperature and heat flux for different mass flow rates and subcooled temperatures. Increasing the mass flow rate requires a higher heat flux and excess temperature for nucleated boiling to occur. Increasing subcooling also needs an increase in heat flux and excess temperature for the appearance of the first vapor bubbles.

Surface roughness also has relevance to the initiation of nucleated boiling. Sun et al [14] showed that increasing roughness decreases the excess temperature required for the ONB.

There are several options for determining the onset nucleated boiling, experimentally. The most widely used, by the scientific community, is checking the point at which the boiling curve departs from the line of forced convection. Another method is the direct observation to detect the formation of the first bubbles. Some authors use the point where the temperature graph of the heated surface stops increasing, becoming constant or even decreasing a few degrees. Pressure drop fluctuations are also considered as a factor to experimentally determine the onset of nucleated boiling.

Kandlikar et al [15] carried out a study on the oscillations of the pressure drop in microchannels as a function of the flow orientation. Some authors have concluded that increased pressure, due to the existence of vapor bubbles, can decrease and reverse the flow.

In the literature there are some correlations to predict the onset of nucleated boiling. However, the boiling phenomenon is dependent on the conditions in which it occurs and, therefore, it is difficult to conclude which correlation to use.

Hsu [16] showed a correlation that admits a minimum excess temperature for nucleated boiling onset.

$$q"_{ONB} = \frac{k_{liq} h_{fg} \rho_v (T_s - T_{sat})^2}{12.8 \theta T_{sat}} \tag{1}$$

Bergles and Rohsenow [3] did extensive studies with water and defined the following correlation.

$$(T_s - T_{sat})_{ONB} = 0,556 \Big[\frac{q"}{1082 p^{1,156}} \Big]^{0,463 p^{0,0234}} \tag{2}$$

The Davis and Anderson [17] model for determining the onset of nucleated boiling is based on the same analytical solution that gave origin to the Bergles and Rohsenow correlation but the static contact angle was added as a factor for the onset of nucleation.

$$(T_s - T_{sat})^2_{ONB} = \frac{8(1 + cos\theta)C}{k_{liq}} q" \tag{3}$$

Where C is determined by

$$C = \frac{\sigma T_{sat}}{\rho_l h_{fg}} \tag{4}$$

Kandlikar et al [18] fitted Hsu's correlation to determine the minimum excess temperature for the onset of nucleated boiling.

$$q"_{ONB} = \frac{k_{liq} h_{fg} \rho_v (T_s - T_{sat})^2}{8.8 \theta T_{sat}} \tag{5}$$

Basu et al [12] created the following correlation, based on data taken from experiments carried out with water, R-113 and R-11 over different metal surfaces.

$$(T_s - T_{sat})_{ONB} = \frac{2 \sigma T_{sat}}{R^*_C F \rho_v h_{fg}} \tag{6}$$

Where R^*_C and F are determined by

$$R^*_C = \Big(\frac{2 \sigma T_{sat} k_{liq}}{h_{fg} q" \rho_v} \Big)^2_{ONB} \tag{7}$$

$$F = 1 - exp\Big[- \Big(\frac{\pi \theta}{180} \Big)^3 - 0,5 \Big(\frac{\pi \theta}{180} \Big) \Big] \tag{8}$$

The studies performed by Basu et al covered surface-liquid pairs with static contact angles between 1 and 85°.

Kandlikar [19] presented the following equation to determine the heat flux required for the onset of nucleated boiling for flows in mini and microchannels.

$$q"_{ONB} = \frac{k_{liq} sen\theta}{1,1 r_c} \Big[(T_s - T_{sat}) - \frac{2 \sigma T_{sat} sin\theta}{h_{fg} \rho_v r_c} \Big] \tag{9}$$

Hong et al [13] presented a correlation for microchannels where one of the relevant parameters is the microchannel height, H, which was considered the characteristic length for the calculation of the Reynolds number, Re.

$$(\Delta T^*_e)_{ONB} = 0,05 Re^{0,156} \Big(\frac{\rho_v}{\rho_l} \Big)^{-0,413} q^{*1,321}_{ONB} \tag{10}$$

Where $(\Delta T^*_e)_{ONB}$ defined as dimensionless excess temperature and q^*_{ONB} defined as dimensionless heat flux, are determined by

$$(\Delta T_e^*)_{ONB} = \frac{(\Delta T_e)_{ONB}}{T_{sat}} = \frac{(T_s - T_{sat})_{ONB}}{T_{sat}} \quad (11)$$

$$q^*_{ONB} = \frac{q"_{ONB}}{G h_{lv}} \quad (12)$$

G represents the mass flow flux.

3. Implementation

3.1. Experimental loop

To assess the critical conditions required for the incipience of nucleate boiling, a test section was added to the experimental installation developed by Nikulin [20] e Andrade [21]. With the addition of the test section, the experimental loop reproduced the operation of a water charge air cooler intercooler and allowed optical visualization of the boiling phenomenon.

The experimental system, represented in figure 1, basically consisted of a closed loop for the forced convective flow driven by a pump (4), 5KH36MNA445X from GE. The working fluid, distilled water or a mixture of ethylene glycol with water (50/50 by volume) was added to the experimental setup through a reservoir (1). The system has two valves (2) and (3) to control the mass flow rate inside the experimental loop and a safety valve (13) to release the vapor inside the test section. A Coriolis flow meter (5), mini-Coriflow from Bronkhorst, measures the mass flow rate entering the test section. A development section (6) follows the flow meter, where the liquid can be heated, by Joule effect, using DC current supplied by a DC power supply (14), HY5050EX from Volteq. The test section (7) has thermocouples, pressure sensors and a heat flux sensor connected to a data acquisition system (8), DT9828 from Data Translation. To a computer (9) are connected the data acquisition system and a high speed camera (10), Phantom V4.2 from Vision Research. A variable transformer (11), SV-4A from Hossoni, is used to regulate the tension supplied to the cartridge heater placed inside of the test section. To close the experimental loop, the liquid passes through a heating/cooling system (12).

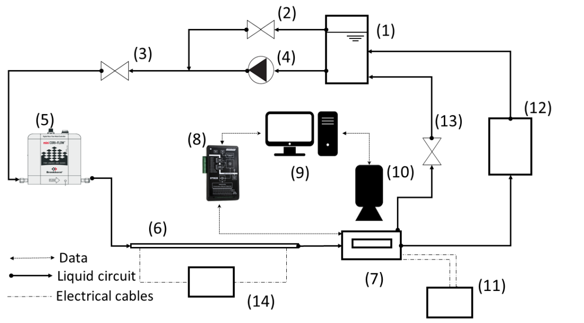

Figure 1: Schematic representation of the experimental set-up: (1) reservoir; (2), (3) and (13) valves; (4) pump; (5) Coriolis flow meter; (6) flow development section; (7) test section; (8) data acquisition system; (9) computer; (10) high speed camera; (11) variable transformer; (12) heating/cooling system; (14) DC power supply

3.2. Test section

The test section, made of 3003 aluminum , was produced to simulate a water charge air cooler and to allow optical visualization of the onset of nucleate boiling which is not possible with a real WCAC intercooler due to its complexity, compactness and number of parts.

Figure 2 shows the test section. It is constituted by three type-k thermocouples (1) and (2) to measure surface and liquid outlet temperatures respectively and a third one to measure the liquid inlet temperature. A cartridge heater (5), from Maxiwatt, is responsible for heating the test surface (7). An adaptor (4) made of copper was used to transform the cylindrical shape of the cartridge heater to a rectangular shape. An insulator made of PTFE was used due to its low thermal conductivity ($k \approx 0,25 W/mK$). Between the cartridge heater and test surface exists a heat flux sensor (6), from Captec. The test section has $120 \times 50 \times 20 mm$ as internal dimensions with a hydraulic diameter $D_h = 28.57 mm$. These dimensions were chosen so that there would be an approximate 2:1 reduction in length and width compared to the single channel dimensions of a WCAC intercooler. The height was increased by about ten times to ensure that the high-speed camera could register the vapor bubbles.

In this study, the test surfaces were made of 3003 aluminum with a thickness of 0.3 mm. However, this test section allows the use of different test surfaces materials and thicknesses.

Connected to the test section is a subsystem responsible for measuring the pressure. This system is composed of two pressure sensors, A-10 from WIKA. One of the sensors measured the inlet pressure while the other measured the outlet pressure. The sensors are connected to a data acquisition system, NI USB-6008 from National Instruments which also collects the data from the heat flux sensor.

Table 1 presents the uncertainties of the equipment used in the experimental setup taking into account the data provided by the manufacturers.

3.3. Procedure

To determine the heat flux and excess temperature required for the ONB, the pump was switched on and the valves adjusted to obtain the desired mass flow rate. Once the mass flow rate value provided

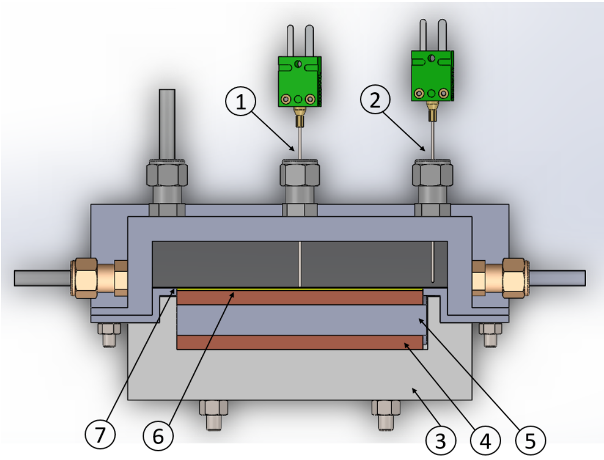

Figure 2: Schematic representation of the test section: (1) and (2) type k thermocouples,(3) insulator; (4) cartridge heater adaptor ; (5) cartridge heater; (6) test surface; (7) heat flux sensor

Table 1: Equipment uncertainties.

Equipamento	Uncertainties
Dektak3 profilometer	± 0.5 [μm]
THETA tensiometer	± 1 [°]
mini-Coriflow flowmeter	± 0.2 [kg/h]
Type K thermocouples	± 0.1 [$°C$]
Hossoni variac	± 1 [V]
WIKA pressure sensor	0.3 [%]
Volteq DC power supply	± 0.015 [V]

by the Coriolis flow meter had stabilised, data collection began. The variable transformer was then turned on so that the cartridge heater would provide heat to the test surface. Initially, 5 V were supplied to the cartridge heater. When the values coming from the heat flux sensor and test surface thermocouple stabilised, more 5 V were added. This process was repeated until reaching the onset of nucleate boiling. Boiling was identified in the course of the tests with the aid of the high-speed camera and, when desired, a video recording was started to capture the boiling phenomenon. After the test, the variable transformer was switched off, data collection was terminated and the cooling system was switched on to bring the working fluid back to its initial conditions

4. Results

In this study, an analysis of the surface properties is carried out, which includes the evaluation of the contact angles of the surfaces with water and with the mixture of water and ethylene glycol (50/50 by volume) and the roughness of the test surfaces. It is performed an assessment to understand if the setup is capable of identifying the ONB using different methods depicted in the literature. A comparison of the boiling onset between water and the mixture of ethylene glycol and water (50/50) is made and the influence of the mass flow rate is studied.

4.1. Wettability

Table 2 shows the results obtained from the wettability and surface tension tests. The average contact angle determined with a tensiometer is shown, as well as its upper and lower deviations. The tests concluded that unbrazed surfaces of aluminium 3003 exhibits a contact angle around of 99° in contact with the mixture of water and ethylene glycol (50/50 by volume) which indicate a hydrophobic behavior and a contact angle around 81° in contact with water which shows a hydrophilic behaviour. The brazed surfaces showed a hydrophilic behavior with both liquids as the measured contact angles were lower than 90°.

A wettability test was performed to the unbrazed surface number 2 after boiling tests. The results showed a decrease in the contact angle. The surface has changed from hydrophobic to hydrophilic behavior as shown in the table 3.

4.2. Roughness

To understand the roughness effect on the critical conditions for the onset of nucleate boiling were performed roughness tests using a profilometer. The results for the average roughness R_a and for the maximum roughness peak to peak R_z are depicted in table 4. The tests were carried out in the longitudinal and transverse direction of the test surfaces. It is possible to observe that the brazing process increased the roughness of the test surfaces by an order of magnitude.

4.3. Thermal losses

As this is a completely new test section developed for the present study, a thermal loss test was carried out. Tests were performed for mass flow rates between $\dot{m} = 3\ kg/h$ and $\dot{m} = 20\ kg/h$ and powers between 100 W e os 600 W.

By observing the figures 3, it possible to see that the heat losses vary between 82% and 47% for mass flow rates between $\dot{m} = 3\ kg/h$ and $\dot{m} = 20\ kg/h$. These values are quite high, but can be explained by the high thermal conductivity ($k = 162\ W/mK$) of the material in which the test section was produced. It is also clear the decrease of thermal losses with the increase of the mass flow rate.

4.4. ONB identifying methods

Different authors use different methods to determine the onset of nucleated boiling as described in 2. In order to understand if the test section and the respective experimental setup is able to reproduce similar behaviours to those shown in the lit-

Table 2: Contact angle and surface tension results.

Property	Surface	Water	Deviation	Mixture	Deviation
Contact Angle [º]	unbrazed 1	99.34	+3.51 -2.05	82.46	+2.10 -1.87
	unbrazed 2	99.51	+2.46 -2.39	81.89	+3.72 -2.70
	unbrazed 3	98.26	+4.01 -3.35	80.53	+3.34 -1.48
	brazed 1	57.95	+7.67 -7.85	53.63	+5.52 -6.18
	brazed 2	56.69	+9.29 -8.05	53.46	+3.62 -4.80
	brazed 3	54.38	+7.91 -7.10	50.62	+8.67 -5.11
Surface Tension [mN/m]	———	72.61	+0.20 -0.27	60.03	+2.01 -1.54

Table 3: Contact angle and surface tension results after boiling test.

Property	Surface	Water	Deviation	Mixture	Deviation
Contact angle [º]	unbrazed 2	57.66	+3.93 -5.51	52.00	+4.17 -2.80

Table 4: Roughness results.

Surface	$R_{a,long}$ $[\mu m]$	$R_{a,trans}$ $[\mu m]$	$R_{z,long}$ $[\mu m]$	$R_{z,trans}$ $[\mu m]$
unbrazed 1	0.268	0.352	1.39	1.95
unbrazed 2	0.338	0.305	1.20	1.06
unbrazed 3	0.237	0.386	1.15	1.35
brazed 1	5.016	3.666	26.2	28.8
brazed 2	6.166	4.776	18.4	18.0
brazed 3	5.468	4.586	20.9	19.1

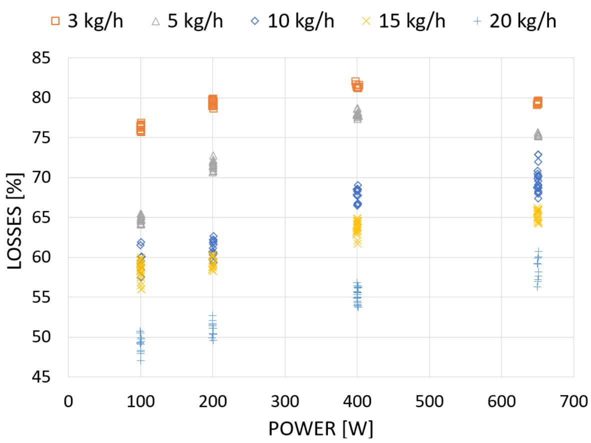

Figure 3: Thermal losses results.

erature, a test was performed using a mixture of ethylene glycol with water (50/50 by volume) with a mass flow rate $\dot{m} \approx 3.5\ kg/h$ and a inlet liquid temperature $T_{in} \approx 25°C$ over an unbrazed test surface.

The figure 4 shows the boiling curve. Looking at the graph one can distinguish between the single-phase flow and the two-phase flow. The ONB is defined at the point where the boiling curve deviates from the forced convection line.

Hong et al [13] identified the ONB at the point where the excess temperature and surface temperature remain constant or decrease. Figure 5 shows the evolution of the excess temperature. Although there was no decrease in the excess temperature, it was found that, at the same point where nucleated boiling starts in the figure 4, graph curve changed its behaviour, where the excess temperature started

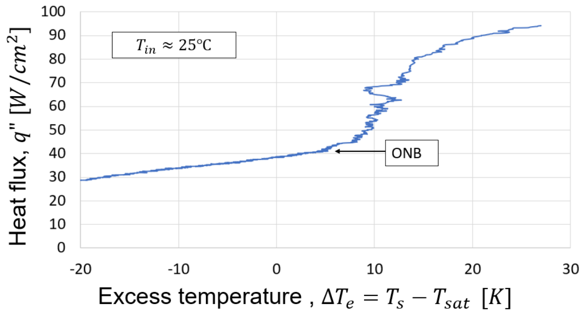

Figure 4: Mixture of ethylene glycol with water 50/50 boiling curve, $\dot{m} \approx 3.5\ kg/h$ and $T_{in} \approx 25°$

to increase less with the increase of heat flux supplied, thus decreasing the slope of graphic curve.

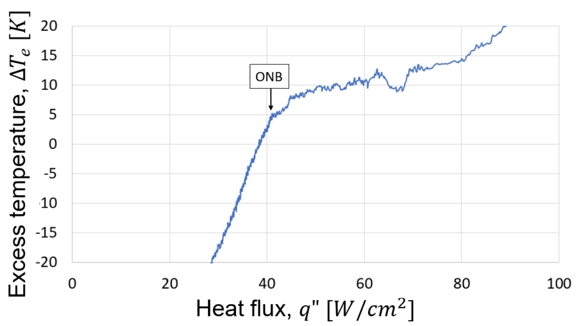

Figure 5: Excess temperature evolution graph, $\dot{m} \approx 3.5\ kg/h$ and $T_{in} \approx 25°$

Another method for experimentally determining nucleated boiling onset was presented by Celata et al [22]. In this method, ONB is identified at point where pressure drop fluctuations increase.

The graph shown in figure 6 shows that two distinct zones can be distinguished, one to the left of the ONB point and the other to the right of the ONB point. On the left it is possible to identify the single phase flow where the pressure drop variations have an amplitude of approximately 0.75 kPa. To the right of point "ONB" it is possible to identify the two-phase flow where the existence of vapor bubbles creates higher pressure drop amplitudes when compared to those of the single-phase flow.

Although it is a less used methodology, the mass flow rate graph can also identify boiling in a flow. As mentioned in section 2, due to the presence of vapor bubbles, the mass flow rate flowing through the test section decreases.

Visually, it was detected that the decrease in mass flow rate only occurred when boiling was in a more developed phase. This can also be demonstrated by the fact that boiling is identified, in the graph in figure 7, by a higher excess temperature when compared to the other methods.

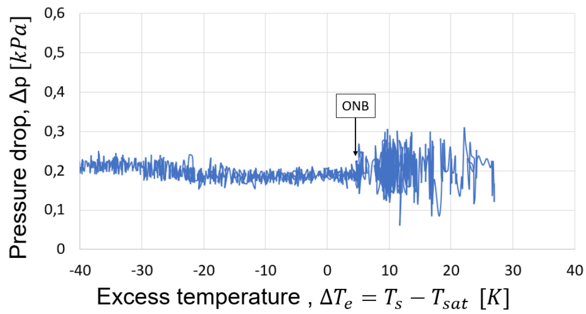

Figure 6: Pressure drop fluctuations graph, $\dot{m} \approx 3.5\ kg/h$ and $T_{in} \approx 25°$

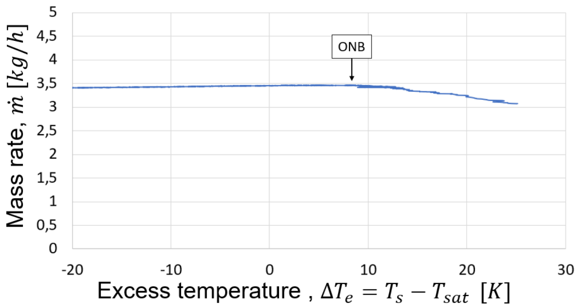

Figure 7: Mass flow rate graph, $T_{in} \approx 25°$

After analysing the data collected, it was found that the inlet pressure sensor also presented variations in its reading. The graph in figure 8 shows the two types of flow. The single-phase flow where the pressure measurements are, practically, constant and with reduced amplitude, i.e. to the left of the ONB point. To the right of the ONB point is the two-phase flow, where both the amplitude of the measured values and the pressure increase due to the existence of vapor bubbles inside the test section. A test was also carried out with water as working fluid to check if the methods for identifying the onset of boiling exhibited the same behaviour. All the methods identified the ONB.

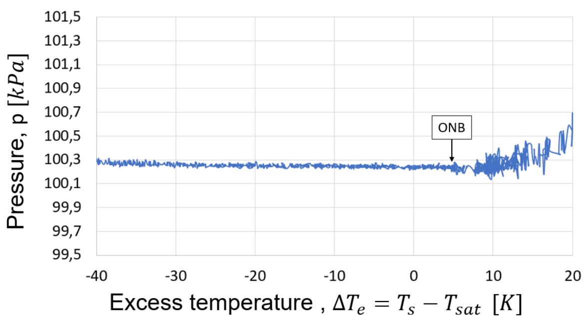

Figure 8: Inlet pressure graph, $\dot{m} \approx 3.5\ kg/h$ and $T_{in} \approx 25°$

4.5. Optical visualization of ONB

With the help of the high-speed camera it was possible to observe different boiling phases. Figure 9 shows The incipience of nucleate boiling. The image was captured during a test with a mass flow rate $\dot{m} \approx 3.5\ kg/h$ and a inlet liquid temperature $T_{in} \approx 25°C$ over an unbrazed surface test. Figure 10 shows a fully developed boiling.

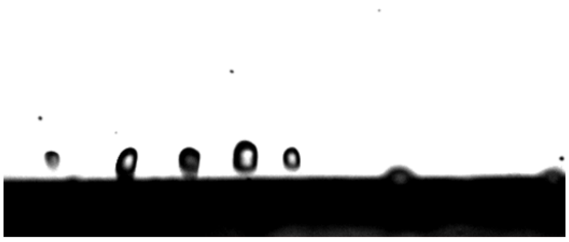

Figure 9: Incipience of nucleate boiling.

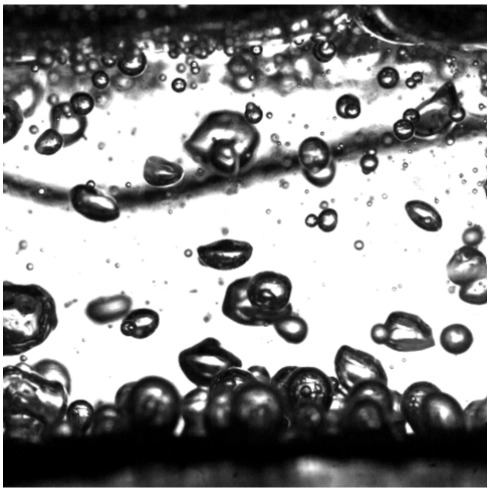

Figure 10: Fully developed boiling.

4.6. Comparison of ONB with water and with mixture of ethylene glycol and water (50/50 by volume)

Figure 11 simultaneously shows the boiling curves of water and the mixture of ethylene glycol and water (50/50 by volume) for a mass flow rate $\dot{m} \approx 3.5kg/h$, an inlet temperature $T_{in} \approx 25°C$ over an unbrazed surface. It can be seen that water initiates boiling for a lower heat flux and excess temperature compared to the mixture. The table 5 presents the values of heat flux and excess temperature at which boiling is initiated on this surface using the different methods described in section 2.

Flow with ethylene glycol mixture started boiling with a heat flux $q"_{ONB} \approx 41\ W/cm^2$ and an excess temperature $\Delta T_{eONB} \approx 5\ K$. With water started with a heat flux $q"_{ONB} \approx 39\ W/cm^2$ and

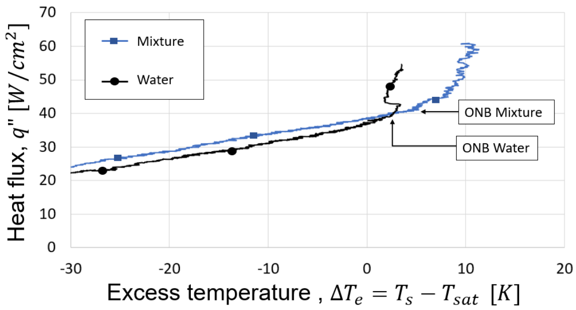

Figure 11: Comparison of ONB with water and with mixture of ethylene glycol and water (50/50) $\dot{m} \approx 3.5\ kg/h$ and $T_{in} \approx 25°$

an excess temperature $\Delta T_{eONB} \approx 2.3\ K$. Four of the five methods showed very similar results. The mass flow rate drop method presented considerably higher values, both for heat flux and excess temperature, for both liquids. This method should be used to understand if boiling exists within a test section, if none of the other methods can be applied.

4.7. Influence of mass flow rate

Table 6 shows the temperature excesses required for nucleated boiling onset. In this case, the changed parameter was the mass flow rate. The tests were performed with a mixture of ethylene glycol with water (50/50 by volume) over an unbrazed surface with an inlet temperature $T_{in} \approx 25°C$

The increase in mass flow rate was translated into the increase in excess temperature required to initiate nucleated boiling, as predicted in the studies by Hong et al [13] and Basu et al [12].

5. Conclusions

In order to evaluate the influence of the wettability, contact angle tests were performed with a tensiometer to characterize the interaction between the surface and liquid. The tests concluded that unbrazed surfaces of aluminium 3003 exhibit a hydrophobic behavior in contact with the mixture of water and ethylene glycol (50/50 by volume) and a hydrophilic behaviour in contact with water. The brazed surfaces showed a hydrophilic behavior with both liquids. The roughness tests exhibited that the brazing process increased the roughness of the test surfaces by an order of magnitude.

The experimental system revealed similar behaviours to those found in the literature with five methods available to identify the onset of nucleate boiling. Of the five methods identified, four showed very similar results for heat flux and excess temperature required for the incipience of boiling.

Onset of nucleate boiling and different boiling phases were identified with a high-speed camera and thus better understand the data taken by the mul-

Table 5: ONB comparison between water and mixture of ethylene glycol and water 50/50 by volume.

	$q"_{ONB}$	$[W/cm^2]$	ΔT_{eONB}	$[K]$
Method	Water	Mixture	Water	Mixture
Boiling curve	39.023	41.093	2.344	5.139
Temperature hysteresis	39.325	41.098	2.361	5.153
Pressure drop fluctuations	38.985	41.107	2.128	5.046
Mass flow rate	42.232	50.125	3.277	9.417
Inlet pressure fluctuations	39.237	41.951	2.397	5.249

Table 6: Results of ONB for different mass flow rates.

Mass flow rate	$\dot{m} \approx 3.5kg/h$	Deviation	$\dot{m} \approx 5kg/h$	Deviation	$\dot{m} \approx 10kg/h$	Deviation
ΔT_{eONB} $[K]$	5.259	0.114	6.538	0.256	8.447	0.411

tiple sensors in the experimental was possible.

Flow boiling tests revealed that the mixture of ethylene glycol and water (50/50 by volume) requires a higher heat flux and a higher excess temperature to initiate boiling, when compared to water for the same mass flow rate, liquid inlet temperature and test surface. They also revealed that increasing the mass flow rate implies an increase in the excess temperature to initiate nucleated boiling.

Acknowledgements

The author would like to thank to professor Ana Moita and professor António Moreira for the support provided, to IN+ for having made available all the necessary resources to carry out this work, to JDeus for providing the necessary materials and a special thanks to the engineers António Amorim, Fernando Oliveira and Luís Neves for their availability and suggestions for improvement throughout this study.

References

[1] Sven Burgold, Jean-Pierre Galland, Benjamin Ferlay, and Laurent Odillard. Modular Water Charge Air Cooling for Combustion Engines. *MTZ worldwide*, 73(11):26–31, 2012.

[2] Shiro Nukiyama. THE MAXIMUM AND MINIMUM VALUES OF THE HEAT Q TRANSMITTED FROM METAL TO BOILING WATER UNDER ATMOSPHERIC PRESSURE*. Technical report.

[3] A. E. Bergles and W. M. Rohsenow. The determination of forced-convection surface-boiling heat transfer. *Journal of Heat Transfer*, 86(3):365–372, 1964.

[4] Satish G. Kandlikar and Murat Bulut. An experimental investigation on flow boiling of ethylene-glycol/water mixtures. *Journal of Heat Transfer*, 125(2):317–325, 2003.

[5] H. S. Lee and Cholewczynski L. W. A Study on Convection and Boiling Heat Transfer Modes in a Standard Engine Cooling System. *International Journal of Heat and Mass Transfer*, 2003.

[6] T.O.N. Andrew. *Experimental Determination of Convection Boiling Curves for Water and Ethylene Glycol in a Rectangular Channel with Localized Heating*. Master's thesis, Western Michigan University, 2005.

[7] Ho Sung Lee and Andrew T. O'Neill. Comparison of boiling curves between a standard S.I. engine and a flow loop for a mixture of ethylene glycol and water. *SAE Technical Papers*, (724), 2006.

[8] Wenhua Yu, David M. France, Dileep Singh, Roger K. Smith, Jason Ritter, Thomas Vijlbrief, and Yves Menger. Subcooled flow boiling of ethylene glycol/water mixtures in a bottom-heated tube. *International Journal of Heat and Mass Transfer*, 72:637–645, 2014.

[9] Gonçalo Gil. *Estudo dos Mecanismos de Ebulição em Permutadores de Calor Líquido / Gás - Water Charge Air Cooler (WCAC)*. Master's thesis, Instituto Superior Técnico, 2020.

[10] Wenhua Yu, David M. France, Dileep Singh, and Weihuan Zhao. Experimental investigation of subcooled flow boiling of a 50/50 ethylene glycol/water mixture in finned rectangular aluminum channels. *Experimental Heat Transfer*, 31(6):482–494, 2018.

[11] Do Yeong Lim, Ji Yong Kim, and In Cheol Bang. Subcooled Flow Boiling with Analysis of Acoustic Signal Behavior. *Department of Nuclear Engineering, Ulsan National Institute of Science and Technology (UNIST*, pages 2–5, 2021.

[12] Nilanjana Basu, Gopinath R. Warrier, and Vijay K. Dhir. Onset of nucleate boiling and active nucleation site density during subcooled flow boiling. *Journal of Heat Transfer*, 124(4):717–728, 2002.

[13] Gang Hong, Xiao Yan, Yan Hua Yang, Shan Liu, and Yan Ping Huang. Experimental study on onset of nucleate boiling in narrow rectangular channel under static and heaving conditions. *Annals of Nuclear Energy*, 39(1):26–34, 2012.

[14] Yan Sun, Li Zhang, Hong Xu, and Xiaocheng Zhong. Subcooled flow boiling heat transfer from microporous surfaces in a small channel. *International Journal of Thermal Sciences*, 50(6):881–889, 2011.

[15] Satish G. Kandlikar and Prabhu Balasubramanian. An experimental study on the effect of gravitational orientation on flow boiling of water in 1054 × 197 μm parallel minichannels. *Journal of Heat Transfer*, 127(8):820–829, 2005.

[16] Y. Y. Hsu. On the size range of active nucleation cavities on a heating surface. *Journal of Heat Transfer*, 84(3):207–213, 1962.

[17] E. J. Davis and G. H. Anderson. The incipience of nucleate boiling in forced convection flow. *AIChE Journal*, 12(4):774–780, 1966.

[18] S. G. Kandlikar. Development of a flow boiling map for suboooled and saturated flow boiling of different fluids inside circular tubes. *Journal of Heat Transfer*, 113(1):190–200, 1991.

[19] Satish G Kandlikar. Nucleation characteristics and stability considerations during flow boiling in microchannels. *Experimental Thermal and Fluid Science*, 30(5):441–447, 2006.

[20] A Nikulin, A S Moita, A L N Moreira, S M S Murshed, A Huminic, Y Grosu, A Faik, J Nieto-maestre, and O Khliyeva. International Journal of Heat and Mass Transfer Effect of Al 2 O 3 nanoparticles on laminar , transient and turbulent flow of isopropyl alcohol. *International Journal of Heat and Mass Transfer*, 130:1032–1044, 2019.

[21] Filipe Arruda Andrade. *Caracterização Experimental da Transmissão de Calor em Escoamentos no Interior de Tubos Corrugados*. Master's thesis, Instituto Superior Técnico, Lisboa, 2018.

[22] Gian Piero Celata, Maurizio Cumo, and Andrea Mariani. Experimental evaluation of the onset of subcooled flow boiling at high liquid velocity and subcooling. *International Journal of Heat and Mass Transfer*, 40(12):2879–2885, 1997.